Nano Research
2019, 12(1): 211–215

ISSN 1998-0124 CN 11-5974/O4
https://doi.org/10.1007/s12274-018-2204-8

Research Article

Ultrathin wavy Rh nanowires as highly effective electrocatalysts for methanol oxidation reaction with ultrahigh ECSA

Xiaoyang Fu[1], Zipeng Zhao[2], Chengzhang Wan[1], Yiliu Wang[1], Zheng Fan[1], Frank Song[1], Bocheng Cao[1], Mufan Li[1], Wang Xue[1], Yu Huang[2,3] (✉), and Xiangfeng Duan[1,3] (✉)

[1] *Department of Chemistry and Biochemistry, University of California, Los Angeles, Los Angeles, California 90095, USA*
[2] *Department of Materials Science and Engineering, University of California, Los Angeles, Los Angeles, California 90095, USA*
[3] *California Nanosystems Institute, University of California, Los Angeles, Los Angeles, California 90095, USA*

Received: 22 May 2018 / **Revised:** 5 September 2018 / **Accepted:** 13 September 2018

ABSTRACT

Direct methanol fuel cells (DMFCs) have received tremendous research interests because of the facile storage of liquid methanol vs. hydrogen. However, the DMFC today is severely plagued by the poor kinetics and rather high overpotential in methanol oxidation reaction (MOR). Here we report the investigation of the ultrathin Rh wavy nanowires as a highly effective MOR electrocatalyst. We show that ultrathin wavy Rh nanowires can be robustly synthesized with 2–3 nm diameters. Electrochemical studies show a current peak at the potential of 0.61 V vs. reversible hydrogen electrode (RHE), considerably lower than that of Pt based catalysts (~ 0.8–0.9 V vs. RHE). Importantly, with ultrathin diameters and favorable charge transport, the Rh nanowires catalysts exhibit an ultrahigh electrochemically active surface area determined from CO-stripping ($ECSA_{CO}$) of 144.2 m^2/g, far exceeding that of the commercial Rh black samples (20 m^2/g). Together, the Rh nanowire catalysts deliver a mass activity of 722 mA/mg at 0.61 V, considerably higher than many previously reported electrocatalysts at the same potential. The chronoamperometry studies also demonstrate good stability and CO-tolerance compared with the Rh black control sample, making ultrathin Rh wavy nanowires an attractive electrocatalyst for MOR.

KEYWORDS

rhodium, nanowires, electrocatalysis, methanol oxidation reaction (MOR)

1 Introduction

Compared with the industrialized hydrogen fuel cells, direct methanol fuel cells (DMFCs) have received tremendous research interests because the storage of methanol is much cheaper and safer compared with that of hydrogen [1]. Additionally, methanol also has a higher volumetric energy density than liquid hydrogen [1]. In particular, the alkaline direct methanol fuel cell (ADMFC) is attracting increasing research interests recently [2]. In alkaline environment, the kinetics of ORR becomes more favorable, which enables the choice of cheaper ORR electrocatalysts [2], such as AlN [3] and many carbon-based nanomaterials [4]. The reversed direction of the electro-osmotic drag also lowers the methanol crossover in the cell, leading to higher efficiency [2]. Unlike the hydrogen fuel cells in which the anode hydrogen oxidation reaction is highly kinetically favorable, the anode methanol oxidation reaction (MOR) in DMFCs is much more difficult and typically requires specific electrocatalysts. For example, nanostructured platinum has been widely studied as anode electrocatalysts for MOR in both alkaline and acidic environments with high mass activity (MA) and specific activity (SA) at the current peak (1,236 mA/mg_{Pt} and 1.93 mA/cm^2 for $Pt/Ni(OH)_2$/graphene (alkaline environment) [5], 2,260 mA/mg_{Pt} and 18.2 mA/cm^2 for PtCu nanoframework (alkaline environment) [6], 1,261.5 mA/mg_{Pt} and 2.96 mA/cm^2 for PtPdRuTe (acidic environment) [7], 2,252 mA/mg_{Pt} and 6.09 mA/cm^2 for PtCu nanotube (acidic environment) [8]). However, these current peaks typically appear at very high overpotential like ~ 0.8–0.9 V vs. reversible hydrogen electrode (RHE) [5–8], which is undesirable for practical fuel cell applications since even the most effective cathode ORR electrocatalysts requires ~ 0.9 V vs. RHE to obtain a considerable reducing current for ORR [9]. Therefore, beyond the peak current density, it is essential to develop a catalyst system that can considerably reduce the overpotential.

Rhodium (Rh) as a noble metal, has received tremendous research interests in the field of catalysis, such as hydrogenation [10], hydroformylation [10], hydrodechlorination [11], ammonia-borane hydrolysis [12], CO oxidation [13], NO_x remediation [13, 14], etc. It is also widely involved in electro catalysis of many reactions. Specifically, for MOR, the rhodium is often involved as one component of a binary or ternary electrocatalysts, such as PtRh [15], PdRh [16], PtRhRu [17], PtSnRh [18], and other noble metals like Pt, Pd are also involved because it is generally believed that the oxophilic nature of Rh is helpful for –OH adsorption, which further helps with the removal of the adsorbed CO [15]. However, it has been challenging to significantly lower the over potential of MOR in order to achieve a high oxidation current at lower potential [15–18].

Various Rh nanostructures, such as nanodendrites [19], mesoporous nanoparticles [14] and nanosheets/RGO [20] have been recently explored as electrocatalysts for MOR with respectable performances in alkaline media. Compared with the CV curves of MOR carried out on Pt, those Rh nanocatalysts can significantly lower the overpotential of MOR in terms of the peak current potential (~ 0.6 V vs. RHE compared with ~ 0.8–0.9 V for Pt), which is important for a higher voltage operation to improve the power output in ADMFCs [14, 19, 20]. However, the mass activity and the specific activity

Address correspondence to Yu Huang, yhuang@seas.ucla.edu; Xiangfeng Duan, xduan@chem.ucla.edu

of these nanocatalysts are usually rather low (MA < 300 mA/mg) [14, 19, 20] compared with those of Pt based nanomaterials [5–8] (MA > 1,000 mA/mg), which negates their advantage of lower overpotential for MOR because high mass activity is essential for reducing the usage of noble metal catalysts and therefore minimizing the costs for practical applications.

In general, the mass activity of an electrocatalyst is determined by the specific activity and electrochemically active surface area (ECSA). The Rh-based MOR electrocatalysts typically exhibit a rather low ECSA (~ 43 m^2/g for Rh nanodendrites, Rh ~ 49 m^2/g for nanosheets/RGO, and 50 m^2/g for Rh mesoporous nanoparticle) [14, 19, 20] due to their relatively large size. Therefore, a straightforward way to improve the mass activity is to increase the ECSA by using ultrafine nanostructures. However, ultrafine nanoparticles (e.g., 2 nm) are typically not stable under relatively aggressive electrochemical conditions due to the physical movement/aggregation and Oswald ripening processes. We have recently reported that ultrafine Pt nanowires are highly stable under oxygen reduction conditions and are exhibiting an extraordinary high ECSA up to 118 m^2/g [9]. Previously, our group have synthesized ultrathin wavy Rh nanowires that show excellent performances for the selective oxidation of benzyl alcohol to benzaldehyde [21]. Here we report the exploration of ultrafine wavy Rh nanowires as a highly effective MOR catalyst with ultrahigh ECSA. We propose that the high specific surface area and the rich surface defects [21] of the ultrathin wavy nanowires may promise increased ECSA and thus higher MA in electrocatalysis. Furthermore, the one-dimensional nanowire geometry is also considered to have an intrinsic advantage in charge transport, which is also beneficial to more efficient utilization of the noble metal nanostructures for electrocatalysis. Herein we successfully synthesized the ultrathin (2–3 nm) wavy Rh nanowires and demonstrated that they can work as excellent MOR electrocatalysts in alkaline media. Significantly, with ultrasmall diameter, the Rh NWs exhibit an ultrahigh $ECSA_{CO}$ of 144.2 m^2/g and more than 2.5-fold higher mass activity (722 mA/mg at 0.61 V vs. RHE) compared with the previously reported Rh nanomaterials [14, 19, 20].

2 Experimental

2.1 Chemicals

Sodium hexachlororhodate(III) (Na_3RhCl_6, analytical grade), potassium iodide (KI, ACS reagent, ≥ 99.5%), polyvinylpyrrolidone (PVP, M_W ~ 55,000), sodium ascorbate (NaAA, crystalline, ≥ 98%), ethanol, acetone, hexane and ethylene glycol (EG, anhydrous, 99.8%) were all purchased from Sigma-Aldrich. The commercial Rh black (> 99.9%) was purchased from Alfa Aesar. All the chemicals were used as received without further purification.

2.2 Synthesis of ultrathin Rh nanowires

The synthesis was following the previous research [9]. Briefly, 10 mg of Na_3RhCl_6, 40 mg NaAA, 160 mg PVP and 85 mg KI were dissolved in 1 mL DI water after ultra-sonication. Then 5 mL of EG was added and mixed as a homogenous mixture. Then the vial was heated at 170 °C for 2 h. After cooling under room temperature, the products were collected via centrifugation after the addition of acetone. The products were then washed via ultra-sonication/centrifugation in the solvent combination of ethanol/acetone for 1 time and ethanol/hexane for 2 times. The final products were dispersed in ethanol for further study after ultra-sonication.

2.3 Structural characterizations

The X-ray diffraction (XRD) was tested on a Panalytical X'Pert Pro X-ray Powder Diffractometer with Cu-Kα radiation after drop-casting the ethanol dispersion of ultrathin Rh wavy nanowires onto the glass substrate and drying under room temperature. X-ray photoelectron spectroscopy (XPS) tests were carried out with Kratos AXIS Ultra DLD spectrometer after drying the ethanol dispersion of the sample on the silicon substrate. Transmission electron microscopy (TEM) images were obtained on an FEI T12 transmission electron microscope operated at 120 kV. High resolution TEM images (HRTEM) was taken on FEI TITAN transmission electron microscope operated at 300 kV. The TEM samples were prepared by dropping ethanol dispersion of the sample onto the carbon-coated copper TEM grids. The loading of ultrathin Rh wavy nanowires on the GCE was determined by the inductively coupled plasma-atomic emission spectroscopy (ICP-AES).

2.4 Electrochemical measurements

All the electrochemical tests were carried out via a three-electrode cell system. The working electrode was a glassy carbon electrode (GCE) with a geometry area of 0.196 cm^2 and the counter electrode was a Pt wire. The reference electrode was Hg/HgO (1 M KOH) purchased from CHI152 and all the potential are converted against RHE after the calibration of the reference electrode in H_2-saturated 1 M KOH aqueous solution. In order to fabricate the working electrode, the Rh wavy nanowires were homogeneously dispersed in EtOH after sonication and 10 μL of the ink was drop casted onto the electrode surface. After drying under room temperature, 10 μL Nafion (0.05 wt.‰) was added and waited till dried under room temperature again.

To activate the Rh electrocatalysts, cyclic voltammetry (CV) was performed in Ar-saturated 1 M KOH electrolyte with a scan rate of 50 mV/s for 50 segments ranging from 0.05 to 1.1 V vs. RHE. The electrochemically active surface area determined from hydrogen under potential deposition ($ECSA_{Hupd}$) was calculated from integrating hydrogen desorption charge from the last cycle of the CV curve using the constant of 220 μC/cm^2 for the hydrogen monolayer.

MOR tests were carried out in Ar-saturated 1 M KOH, 1 M MeOH electrolyte with potential scan rate of 50 mV/s. The chronoamperometry tests were carried out at 0.52 V vs. RHE for 6,000 s.

The CO-stripping tests were also carried out to determine the $ECSA_{CO}$. After activation in Ar-saturated 1 M KOH via CV, the GCE was dipped into CO-saturated 1 M KOH electrolyte for allowing the CO to be adsorbed onto the Rh as monolayer. The electrolyte was then changed to Ar-saturated 1 M KOH and CO-stripping test was carried out with potential scan rate of 50 mV/s. The metal loading of Rh nanowires on the electrode determined from ICP-AES was 0.880 μg (4.49 μg/cm^2 normalized over the geometric area of the GCE) and the value of currents were normalized by the mass of the Rh loading on the electrode. The commercial Rh black was also tested as control under the same conditions with a mass loading of 1.0 μg (5.1 μg/cm^2).

3 Results and discussion

3.1 Characterizations of ultrathin Rh nanowires

The morphologies of the ultrafine wavy Rh nanowires were studied by transmission electron microscope (TEM). TEM image clearly demonstrates ultrafine wavy nanowire geometry with diameters of about 2–3 nm and lengths exceeding 200 nm (Fig. 1(a)), which agrees well with the previous literature [21]. The high-resolution TEM (HRTEM) image shows clearly resolved lattice fringes with a lattice spacing of 0.22 nm (Fig. 1(b) and inset), corresponding to the (111) lattice planes of the FCC Rh, which is also consistent with previous literatures [14, 19–21]. There are also apparently many surface defects as observed in the previous literature, which represents the catalytic active sites for selective oxidation of benzyl alcohol to benzyl aldehyde [21]. The ultrafine size and rich surface defects may potentially contribute to the electrocatalysis of MOR as well.

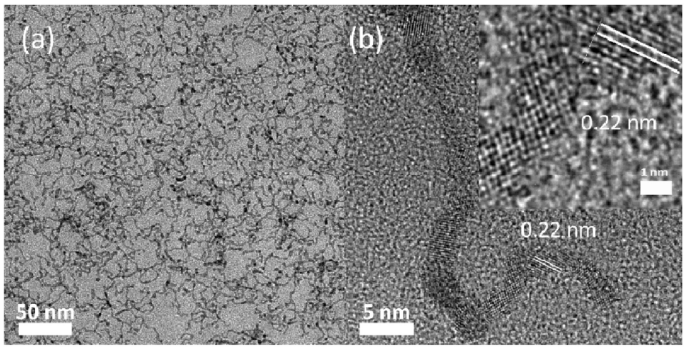

Figure 1 Structural characterizations of the ultrathin Rh wavy nanowires. (a) TEM, (b) HRTEM image.

Figure S1 in the Electronic Supplementary Material (ESM) shows the XRD pattern of the ultrathin wavy Rh nanowire sample, the peaks at 41.1°, 47.7°, 69.9° and 84.4° are corresponding to the (111), (200), (220) and (311) crystal planes of the FCC Rh (JCPDS No. 05-0685), which also agree with the previous literatures [14, 19, 20].

In Fig. S2 in the ESM, the XPS shows the composition and valence of the surficial Rh species. The peaks at the binding energies of 307.3 and 312.1 eV correspond to the $3d_{5/2}$ and $3d_{3/2}$ of the metallic Rh (0) [14, 19, 20], respectively. The peaks at the binding energies of 308.3 and 313.1 eV correspond to the $3d_{5/2}$ and $3d_{3/2}$ of the Rh (III) [14, 19, 20] which may result from the oxidized surficial Rh in air and the unreacted residue precursor. The peak area ratio of $3d_{5/2}$ and $3d_{3/2}$ follows the theoretical value of 3:2 for both Rh (0) and Rh (III) and the content of the Rh (0) is calculated as 69.8% from the peak area.

3.2 Electrocatalytical methanol oxidation reaction

The electrochemical performances of the Rh nanowire catalysts were first studied via CV to determine the $ECSA_{Hupd}$ (Fig. 2(a) dotted line). In the 1 M KOH electrolyte without methanol, the forward scan demonstrates two primary peaks corresponding to hydrogen desorption at 0.06–0.35 V [19, 20] and oxygen adsorption at > 0.4 V [19, 21]. The reverse scan also exhibits two primary peaks corresponding to hydrogen adsorption at 0.05–0.27 V [19, 20] and oxygen desorption at 0.43 V [19, 21]. The $ECSA_{Hupd}$ was calculated to be 105.3 m^2/g by using the constant of 220 $\mu C/cm^2$ for the hydrogen monolayer [20, 22] after integration, which is more than 2-fold higher than the $ECSA_{Hupd}$ of Rh nanocatalysts reported previously (Rh nanodendrites: ~ 43 m^2/g, Rh nanosheets/RGO: ~ 49 m^2/g) [19, 20]. The $ECSA_{CO}$ of the Rh nanowires determined from CO-stripping (Fig. 2(a) solid line) by using the constant of 440 $\mu C/cm^2$ for the CO monolayer [22] is 144.2 m^2/g and is 7.2-fold higher than that of the commercial Rh black (20 m^2/g) (Fig. S3 in the ESM). The ultrahigh ECSA mostly likely arises from the high surface to volume ratio and rich surface defects of the ultrathin wavy nanowires [21]. Additionally, the favorable charge transport in the 1D geometry is also beneficial for maximizing the utilization efficiency of the active sites in electrocatalysis. Together, the high ECSA suggests excellent potential of the Rh nanowires as highly effective electrocatalysts.

The catalytic activity of the Rh nanowires for MOR was carried out in the electrolyte of 1 M KOH and 1 M methanol. The forward scan demonstrates a strong current peak at the potential of 0.61 V vs. RHE, corresponding to the oxidation of methanol with a peak mass activity of 722 mA/mg. This mass activity represents the highest value among all the previously reported monometallic Rh nanocatalysts tested at room temperature, including Rh mesoporous nanoparticle (288 mA/mg), Rh nanosheets/RGO (264 mA/mg), Rh nanodendrites (255.6 mA/mg) and is 7.7-fold higher than the commercial Rh black (93.6 mA/mg), and is also higher than many MOR catalysts reported to date at 0.61 V vs. RHE, indicating great utilization efficiency of the noble metal. The peak potential at 0.61 V also generally agrees well with the corresponding values from the previous literatures and may be tentatively attributed to the intrinsic properties of Rh nanomaterials (with a lower peak potential compared with those of Pt-based nanomaterials) [14, 19, 20].

The specific activity is calculated as 0.686 mA/cm^2 based on the $ECSA_{Hupd}$ and this value is slightly higher compared with the previous literatures [19, 20] (Rh nanodendrites: 0.590 mA/cm^2 based on the $ECSA_{Hupd}$, Rh nanosheets: 0.543 mA/cm^2 based on the $ECSA_{Hupd}$), which may be attributed to the low coordination number of Rh in the ultrathin wavy nanowires and the intrinsic advantage of charge transport of the nanowires [9, 21]. We can tentatively conclude that the high mass activity of the Rh wavy nanowires largely arises from the ultrahigh ECSA since the specific activity is not greatly improved.

In the reverse scan the anodic peak has a negative potential shift and lower current compared with those in the forward scan, this phenomenon has also been widely observed with Pt-based nanomaterials during MOR. According to the most recent literatures, this hysteresis phenomenon on the Pt-based nanomaterials during MOR is explained as the change of rate-determining-step from water dissociation step to methanol dehydrogenation step during the reverse scan since the oxygenated species are adsorbed onto the Pt surface after the forward scan, which makes the current peak potential and peak current different in the reverse scan [23, 24]. The I_F/I_R demonstrates the oxophilicity of the catalyst and lower I_R indicates the electrocatalysts surface are occupied by more oxygenated species which demonstrates higher oxophilicity [23, 24]. The I_F/I_R of the ultrathin Rh wavy nanowires is ~ 2.3, which is higher compared with some of the previously reported Pt-based nanomaterials with $I_F/I_R < 2$ [7, 8, 12, 25], indicating comparably higher oxophilicity.

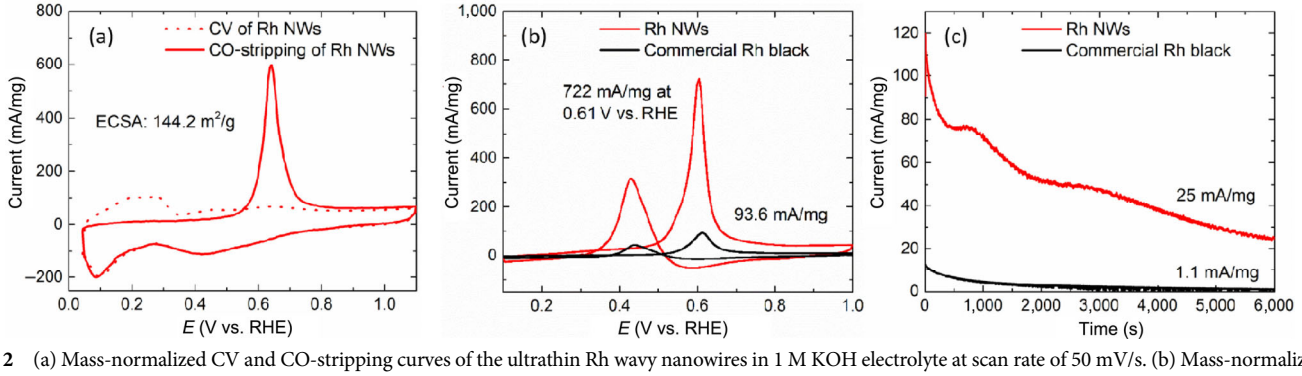

Figure 2 (a) Mass-normalized CV and CO-stripping curves of the ultrathin Rh wavy nanowires in 1 M KOH electrolyte at scan rate of 50 mV/s. (b) Mass-normalized CV curves of the ultrathin Rh wavy nanowires and commercial Rh black in 1 M KOH + 1 M MeOH electrolyte at scan rate of 50 mV/s. (c) Chronoamperometry results of the ultrathin Rh wavy nanowires and commercial Rh black in 1 M KOH +1 M MeOH electrolyte at 0.52 V vs. RHE.

This also agrees with the volcano plot, in which Rh binds more easily to OH and oxygen [16, 26], which also indicates that the Rh is considered to be more oxophilic than Pt.

The chronoamperometry tests (Fig. 2(c)) were carried out to demonstrate the stability of the Rh nanowire electrocatalyst during long time of operation [20, 23, 24]. The ultrathin wavy Rh nanowire is able to retain a current of 25 mA/mg at 0.52 V vs. RHE after 6,000 s. This value is much higher than commercial Rh black and generally comparable with the previous literatures [14, 19], which indicates acceptable stability and CO-tolerance.

3.3 Comparison with previously reported Pt-based electrocatalysts

For the Pt-based nanomaterials, despite of the ultrahigh mass activity, the current peak appears at much higher potential [5–8] (~ 0.8–0.9 V vs. RHE.), which may not be really applicable for DMFCs since it is close to the half-wave potential of the cathode ORR eletrocatalysts [9]. The mass activity of many previously reported Pt-based nanomaterials at 0.61 V vs. RHE are also lower than that obtained with the Rh nanowires (Fig. 3) [5, 6, 14, 19, 20, 27]. The comparison in Fig. 3 clearly demonstrates that Rh nanowires exhibit a favorable combination of high mass activity and lower overpotential.

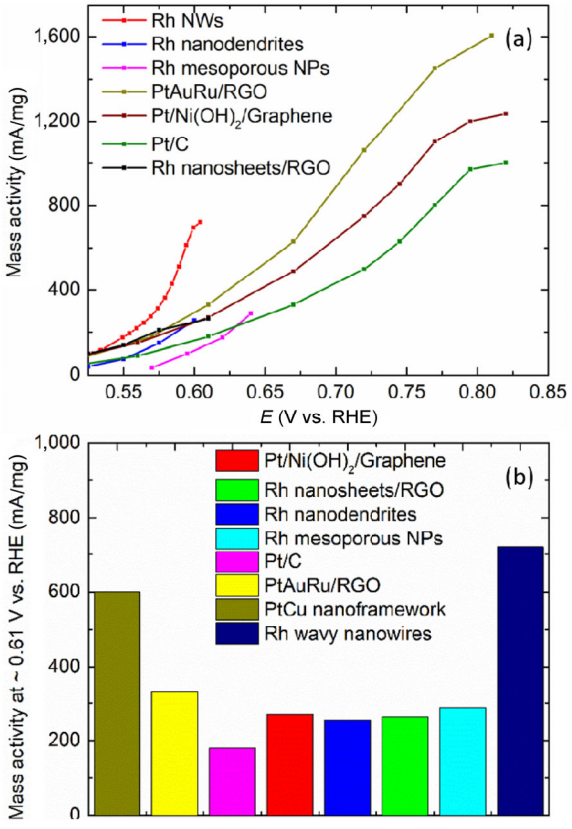

Figure 3 (a) Summary of various previously reported Rh and Pt-based electrocatalysts tested in the electrolyte of 1M MeOH + 1M KOH regarding their mass activities at different potentials. (b) The MOR mass activity at ~ 0.61 V vs. RHE of the Rh and Pt-based electrocatalysts tested in alkaline media.

4 Conclusion

In summary, we have shown that ultrathin Rh wavy nanowires can function as highly effective MOR catalysts with low overpotential and ultrahigh ECSA, together delivering a mass activity of 722 mA/mg at 0.61 V vs. RHE, which is higher than most of the previously reported eletrocatalyst at the same potential. Therefore, we believe the ultrathin wavy Rh nanowires may represent a highly promising electrocatalyst for MOR.

Acknowledgements

We acknowledge support from the Office of Naval Research Office under the grant number N00014-18-1-2491.

Electronic Supplementary Material: Supplementary material (XRD and XPS characterizations of Rh nanowires and CO-stripping study of the commercial Rh black) is available in the online version of this article at https://doi.org/10.1007/s12274-018-2204-8.

References

[1] Joghee, P.; Malik, J. N.; Pylypenko, S.; O'Hayre, R. A review on direct methanol fuel cells–In the perspective of energy and sustainability. *MRS Energy Sustain.* **2015**, *2*, E3.

[2] Yu, E. H.; Krewer, U.; Scott, K. Principles and materials aspects of direct alkaline alcohol fuel cells. *Energies* **2010**, *3*, 1499–1528.

[3] Lei, M.; Wang, J.; Li, J. R.; Wang, Y. G.; Tang, H. L.; Wang, W. J. Emerging methanol-tolerant AlN nanowire oxygen reduction electrocatalyst for alkaline direct methanol fuel cell. *Sci. Rep.* **2014**, *4*, 6013.

[4] Wang, D.-W.; Su, D. S. Heterogeneous nanocarbon materials for oxygen reduction reaction. *Energy Environ. Sci.* **2014**, *7*, 576–591.

[5] Huang, W. J.; Wang, H. T.; Zhou, J. G.; Wang, J.; Duchesne, P. N.; Muir, D.; Zhang, P.; Han, N.; Zhao, F. P.; Zeng, M. et al. Highly active and durable methanol oxidation electrocatalyst based on the synergy of platinum–nickel hydroxide–graphene. *Nat. Commun.* **2015**, *6*, 10035.

[6] Zhang, Z. C.; Luo, Z. M.; Chen, B.; Wei, C.; Zhao, J.; Chen, J. Z.; Zhang, X.; Lai, Z. C.; Fan, Z. X.; Tan, C. L. et al. One-pot synthesis of highly anisotropic five-fold-twinned PtCu nanoframes used as a bifunctional electrocatalyst for oxygen reduction and methanol oxidation. *Adv. Mater.* **2016**, *28*, 8712–8717.

[7] Ma, S. Y.; Li, H. H.; Hu, B. C.; Cheng, X.; Fu, Q. Q.; Yu, S. H. Synthesis of low Pt-based quaternary PtPdRuTe nanotubes with optimized incorporation of Pd for enhanced electrocatalytic activity. *J. Am. Chem. Soc.* **2017**, *139*, 5890–5895.

[8] Li, H. H.; Fu, Q. Q.; Xu, L.; Ma, S. Y.; Zheng, Y. R.; Liu, X. J.; Yu, S. H. Highly crystalline PtCu nanotubes with three dimensional molecular accessible and restructured surface for efficient catalysis. *Energy Environ. Sci.* **2017**, *10*, 1751−1756.

[9] Li, M. F.; Zhao, Z. P.; Cheng, T.; Fortunelli, A.; Chen, C. Y.; Yu, R.; Zhang, Q. H.; Gu, L.; Merinov, B. V.; Lin, Z. Y. et al. Ultrafine jagged platinum nanowires enable ultrahigh mass activity for the oxygen reduction reaction. *Science* **2016**, *354*, 1414–1419.

[10] Guerrero, M.; Than Chau, N. T.; Noël, S.; Denicourt-Nowicki, A.; Hapiot, F.; Roucoux, A.; Monflier, E.; Philippot, K. About the use of rhodium nanoparticles in hydrogenation and hydroformylation reactions. *Curr. Org. Chem.* **2013**, *17*, 364–399.

[11] Cobo, M.; Becerra, J.; Castelblanco, M.; Cifuentes, B.; Conesa, J. A. Catalytic hydrodechlorination of trichloroethylene in a novel NaOH/2-propanol/methanol/water system on ceria-supported Pd and Rh catalysts. *J. Environ. Manage.* **2015**, *158*, 1–10.

[12] Wang, L. B.; Li, H. L.; Zhang, W. B.; Zhao, X.; Qiu, J. X.; Li, A. W.; Zheng, X. S.; Hu, Z. P.; Si, R.; Zeng, J. Supported rhodium catalysts for ammonia–borane hydrolysis: Dependence of the catalytic activity on the highest occupied state of the single rhodium atoms. *Angew. Chem., Int. Ed.* **2017**, *56*, 4712–4718.

[13] Parry, I. S.; Kartouzian, A.; Hamilton, S. M.; Balaj, O. P.; Beyer, M. K.; Mackenzie, S. R. Collisional activation of N_2O decomposition and CO oxidation reactions on isolated rhodium clusters. *J. Phys. Chem. A* **2013**, *117*, 8855–8863.

[14] Jiang, B.; Li, C. L.; Dag, Ö.; Abe, H.; Takei, T.; Imai, T.; Hossain, M. S. A.; Islam, M. T.; Wood, K.; Henzie, J. et al. Mesoporous metallic rhodium nanoparticles. *Nat. Commun.* **2017**, *8*, 15581.

[15] Li, L.; Tian, C. X.; Yang, J. S.; Zhang, X. H.; Chen, J. H. One-pot synthesis of PtRh/β-CD-CNTs for methanol oxidation. *Int. J. Hydrogen Energy* **2015**, *40*, 14866–14874.

[16] Jurzinsky, T.; Bär, R.; Cremers, C.; Tübke, J.; Elsner, P. Highly active carbon supported palladium-rhodium Pd_xRh/C catalysts for methanol electrooxidation in alkaline media and their performance in anion exchange direct methanol fuel cells (AEM-DMFCs). *Electrochim. Acta* **2015**, *176*, 1191–1201.

[17] Chotkowski, M.; Uklejewska, M.; Siwek, H.; Dłubak, J.; Czerwiński, A. Characterization of Pt–Rh–Ru catalysts for methanol oxidation. *Funct. Mater. Lett.* **2011**, *4*, 187–191.
[18] Jiang, K. Z.; Bu, L. Z.; Wang, P. T.; Guo, S. J.; Huang, X. Q. Trimetallic PtSnRh wavy nanowires as efficient nanoelectrocatalysts for alcohol electrooxidation. *ACS Appl. Mater. Interfaces* **2015**, *7*, 15061–15067.
[19] Kang, Y. Q.; Li, F. M.; Li, S. N.; Ji, P. J.; Zeng, J. H.; Jiang, J. X.; Chen, Y. Unexpected catalytic activity of rhodium nanodendrites with nanosheet subunits for methanol electrooxidation in an alkaline medium. *Nano Res.* **2016**, *9*, 3893–3902.
[20] Kang, Y. Q.; Xue, Q.; Jin, P. J.; Jiang, J. X.; Zeng, J. H.; Chen, Y. Rhodium nanosheets–reduced graphene oxide hybrids: A highly active platinum-alternative electrocatalyst for the methanol oxidation reaction in alkaline media. *ACS Sustain. Chem. Eng.* **2017**, *5*, 10156–10162.
[21] Huang, X. Q.; Zhao, Z. P.; Chen, Y.; Chiu, C. Y.; Ruan, L. Y.; Liu, Y.; Li, M. F.; Duan, X. F.; Huang, Y. High density catalytic hot spots in ultrafine wavy nanowires. *Nano Lett.* **2014**, *14*, 3887–3894.
[22] Durst, J.; Simon, C.; Hasché, F.; Gasteiger, H. A. Hydrogen oxidation and evolution reaction kinetics on carbon supported Pt, Ir, Rh, and Pd electrocatalysts in acidic media. *J. Electrochem. Soc.* **2015**, *162*, F190–F203.
[23] Hofstead-Duffy, A. M.; Chen, D. J.; Sun, S. G.; Tong, Y. J. Origin of the current peak of negative scan in the cyclic voltammetry of methanol electro-oxidation on Pt-based electrocatalysts: A revisit to the current ratio criterion. *J. Mater. Chem.* **2012**, *22*, 5205–5208.
[24] Chung, D. Y.; Lee, K. J.; Sung, Y. E. Methanol electro-oxidation on the Pt surface: Revisiting the cyclic voltammetry interpretation. *J. Phys. Chem. C* **2016**, *120*, 9028–9035.
[25] Mikkelsen, K.; Cassidy, B.; Hofstetter, N.; Bergquist, L.; Taylor, A.; Rider, D. A. Block copolymer templated synthesis of core–shell PtAu bimetallic nanocatalysts for the methanol oxidation reaction. *Chem. Mater.* **2014**, *26*, 6928–6940.
[26] Nørskov, J. K.; Rossmeisl, J.; Logadottir, A.; Lindqvist, L.; Kitchin, J. R.; Bligaard, T.; Jónsson, H. Origin of the overpotential for oxygen reduction at a fuel-cell cathode. *J. Phys. Chem. A* **2004**, *108*, 17886–17892.
[27] Ren, F. F.; Wang, C. Q.; Zhai, C. Y.; Jiang, F. X.; Yue, R. R.; Du, Y. K.; Yang, P.; Xu, J. K. One-pot synthesis of a RGO-supported ultrafine ternary PtAuRu catalyst with high electrocatalytic activity towards methanol oxidation in alkaline medium. *J. Mater. Chem. A* **2013**, *1*, 7255–7261.